First Passage Time Statistics For Systems Driven by Long Range Gaussian Noises

Aldo H. Romero

Facultad de Física, Pontificia Universidad Católica de Chile, Casilla 306, Santiago 22, Chile

J. M. Sancho

Departament d'Estructura i Constituents de la Matéria,
Universitat de Barcelona, Av. Diagonal 647, 08028 Barcelona. Spain

Katja Lindenberg

Department of Chemistry and Biochemistry and Institute for Nonlinear Science,
University of California San Diego, 9500 Gilman Drive, La Jolla, California 92093-0340, USA

We examine the mean first passage time for a particle driven by highly correlated Gaussian fluctuations to reach one or more predetermined boundaries. We discuss a numerical algorithm to generate power-law correlated fluctuations and apply these to three physical examples. One is the arrival of a free particle at either end of an interval. The second is the decay of a particle from an unstable state. The third is the time for a particle to cross a barrier separating one well from another in a double well potential. In each case a comparison with the first passage time for a particle driven by Gaussian white noise is presented, as is an analysis of the dependence of the first passage time properties on the correlated noise parameters.

I. INTRODUCTION

The arrival of a random process at a particular state often triggers some important behavior. Among the large number of instances that one can name are the firing of a neuron, the nucleation of a phase associated with a phase transition, the triggering of an alarm, the occurrence of a major earthquake, and the crossing of an activation barrier by a reaction coordinate that converts reactants to products in a chemical reaction. These examples range from the macroscopic to the microscopic, indicating that the arrival problem is of interest on all scales. In many instances it is not only important to know the statistics of occurrence of such events, but more specifically the statistics of *first* occurrence. This then leads to the study of the statistical properties of the time that it takes a random process to reach a specified state for the first time, that is, the *mean first passage time*. The first passage time literature is enormous and extends over many decades [1, 2, 3, 4, 5].

For simplicity we restrict our attention in this work to one-dimensional random processes $x(t)$, although the generalization to vector processes or even to fields is conceptually straightforward. The statistical properties of the temporal evolution of the random process are typically described in one of two ways. One is by way of an evolution equation for the probability distribution $P(x, t)$ for the random variable to take on the value $x(t) = x$ at time t (the random variable and the values that it can take on are often denoted by the same symbol, x in this case, although the distinction should be kept in mind). The other is by way of an evolution equation ("Langevin equation") for the random variable itself. From the solution of the appropriate evolution equation (via steps that are in general non-trivial) one can then obtain the first passage time statistics for $x(t)$ to reach a prescribed value for the first time. In either case, one often thinks of the evolution of $x(t)$ as being driven by fluctuations $\eta(t)$ of prescribed statistical properties from which the statistics of $x(t)$ then follow.

Let us then turn to the "driving fluctuations" $\eta(t)$ and their typical statistical properties. By far the most common assumption is that fluctuations have a Gaussian distribution, although there has always been a great deal of interest in fluctuations that are distributed in some other fashion. The most common examples include Lévy distributions [6, 7] (distributions with very long tails), and dichotomous processes [8, 9] (where the random variable can take on only two values). The former typically arise when the fluctuations are a result of many multiplicative inputs; the latter often serve as an analytically tractable prototype.

In order to specify the fluctuations fully, one must also explicitly state their correlation properties. If they are Gaussian,

$$P(\eta) = \frac{1}{\sqrt{2\pi}\sigma} e^{-\eta^2/2\sigma^2}, \tag{1}$$

then only the average $\langle \eta(t) \rangle$ (usually and here as well taken to be zero) and two-time correlation function (assumed stationary) $\gamma(t - t') \equiv \langle \eta(t)\eta(t') \rangle$ need to be specified, since all other correlation properties then follow. In Eq. (1) $\sigma^2 = \gamma(0)$. For other distributions it is in general necessary to also specify higher order correlations functions, even

though these are often difficult to determine. The early literature dealt primarily with δ- correlated or "white noise" processes,

$$\gamma(t) = 2D\delta(t) \tag{2}$$

and D (the integral of the correlation function) measures the intensity of the noise. In this case the second moment σ^2 diverges as $D/\Delta t$, where $\Delta t \to 0$ is the "width" of the δ-function and therefore the shortest time scale in the problem. The evolution equation $P(x,t)$ for a random process driven by Gaussian δ-correlated fluctuations $\eta(t)$ is the familiar Fokker-Planck equation [1, 4], and the associated first passage time properties are well understood [1, 4, 10].

About two decades ago a great deal of attention began to be directed toward understanding the effects of "colored noise", that is, of driving fluctuations that are not δ-correlated. Most of the attention was focused on *exponentially correlated* noise,

$$\gamma(t) = \frac{D}{\tau}e^{-|t|/\tau}, \tag{3}$$

where τ is the correlation time of the noise. The associated evolution equation for $P(x,t)$ and related first passage time properties as a function of the correlation time were studied in detail and are also well understood [11]. For instance, it is firmly established that the mean first passage time from one potential well to another of a process $x(t)$ driven by exponentially correlated noise increases with increasing correlation time. It is also understood that the particular exponential form of the correlation function is not crucial in the qualitative features of the first passage time statistics. The most important feature determining the qualitative features of the first passage time statistics is the fact that there is a *finite* correlation time associated with the fluctuations.

More recently there has been considerable interest in (typically Gaussian) fluctuations that display long-range power-law correlations with an infinite correlation time. Such highly correlated fluctuations have been considered in a broad array of circumstances ranging from the biological to the physical, from the economical to the atmospheric, and encompassing theoretical and experimental studies [12, 13]. There are two separate issues that need to be addressed with such highly correlated noise. One is the numerical generation of the correlated noise itself. Only recently have the traditional Fourier filtering methods been superseded by far more efficient procedures [12, 14, 15, 16, 17] that will briefly be reviewed below in the context of our systems. The second issue is that of the effect of such a driving noise on the first passage time properties of the system that is driven by these highly correlated fluctuations, and this is our principal interest in this paper. Herein we examine the mean first passage time of a particle, driven by highly correlated fluctuations, in three different physical situations. In the first case, we discuss the arrival of a free particle (moving superdiffusively) at an absorbing boundary. As a second case, we study the decay of a particle from an initial unstable state. Finally, we discuss the time for a particle to cross a barrier separating one well from the other in a double well potential.

In Sec. II we summarize the main steps in the generation of long ranged correlated Gaussian noises. In Secs. III, IV, and V we present respectively the arrival of the superdiffusive particle at an absorbing boundary, the decay of an unstable state, and the barrier crossing problem. Finally, we conclude with a summary in Sec. VI.

II. GENERATION OF LONG RANGE CORRELATED GAUSSIAN NOISE

The main steps to generate noises with a Gaussian distribution and arbitrary correlation properties can be found in Refs. [12, 14, 15, 16, 17]. Here we present a summary of these "spectral methods" including some details relevant to our applications. The goal is to generate a Gaussian noise $\eta(t)$, with correlation function $\gamma(t)$ defined by:

$$\langle \eta(t)\eta(t')\rangle = \gamma(t - t'), \tag{4}$$

and with a Fourier transform

$$\widetilde{\gamma}(\omega) = \int_{-\infty}^{\infty} dt\, e^{-i\omega t}\gamma(t). \tag{5}$$

This correlation function may be specified analytically or numerically. In the ω Fourier-space, the transformed noise $\widetilde{\eta}(\omega)$ has a correlation function

$$\langle \widetilde{\eta}(\omega)\widetilde{\eta}(\omega')\rangle = 2\pi\gamma(\omega)\delta(\omega + \omega'). \tag{6}$$

The algorithm for the noise generation can be summarized as follows. First, the time interval $(0, t)$ is discretized into $N = 2^n$ intervals of mesh size Δt. This time interval has to be much smaller than any other characteristic time
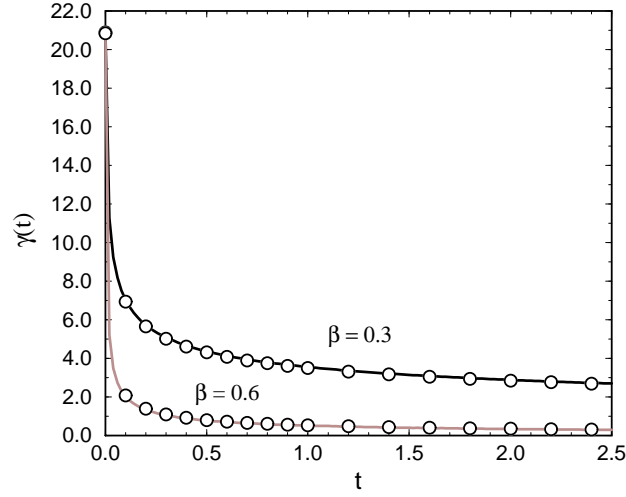
FIG. 1: Comparison of Eq. (15) (circles) with correlation functions generated with the algorithm described in the text (solid lines). Upper curve: $\beta = 0.3$ with $t_0 = 0.0026$. Lower curve: $\beta = 0.6$ with $t_0 = 0.0022$. Other parameters for both curves: $\epsilon = 20.0$, $N = 2^{19}$, $\Delta t = 0.01$, $\omega_0 = 0.0001$. These simulation results are averaged over 100 realizations.
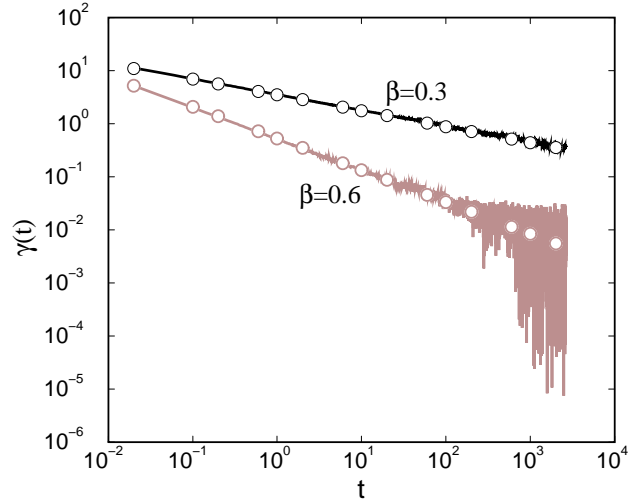

FIG. 2: Same as Fig. 1but on a logarithmic scale that highlights the power law behavior.

of the system (and hence N must be sufficiently large) because it is used as the time integration step in the numerical simulation of the stochastic evolution equations. The intervals in time will be denoted by a roman index and the resulting frequency intervals in Fourier space are denoted by a greek index. In discrete Fourier space the noise has a correlation function given by

$$\langle \widetilde{\eta}(\omega_\mu)\widetilde{\eta}(\omega_{\mu'}) \rangle = N\Delta t \widetilde{\gamma}(\omega_\mu)\delta_{\mu+\mu',0}, \tag{7}$$

where $\widetilde{\eta}(\omega_\mu)$ can be constructed as follows:

$$\widetilde{\eta}(\omega_\mu) = \sqrt{N\Delta t \widetilde{\gamma}(\omega_\mu)} \, \alpha_\mu, \quad \mu = 0, \dots, N-1$$

$$\widetilde{\eta}(\omega_N) = \widetilde{\eta}(\omega_0), \qquad \qquad \omega_\mu = \frac{2\pi\mu}{N\Delta t}.$$

(8)

Here the α_μ are Gaussian random numbers with zero mean and with correlation

$$\langle \alpha_\mu \alpha_\nu \rangle = \delta_{\mu+\nu,0} .$$

(9)

This type of δ-anticorrelated noise can be generated rather easily if the symmetry properties of real periodic series in the Fourier space (α_i) are used [14, 17]. Owing to the periodicity of $\widetilde{\gamma}(\omega_\mu)$, the index μ can be made to run from $-N/2$ to $N/2$, and the maximum frequency is $\omega_{max} = \pi/\Delta t$ [17]. The Fourier components are related by $\alpha_{\mu+pN} = \alpha_\mu$ for any integer p, and $\alpha_{-\mu} = \alpha_\mu^*$ because the original random numbers in time are real. The anticorrelated random numbers can then be constructed as $\alpha_\mu = a_\mu + ib_\mu$ with $b_0 = 0$, $a_0^2 = 1$, and a_μ and b_μ are each Gaussian random numbers with zero mean and a variance of $1/2$ for $\mu \neq 0$.

The discrete inverse transform of any sequence $\widetilde{\eta}(\omega_\mu)$ is then numerically calculated by a standard Fast Fourier Transform algorithm. The result is a string of N numbers, $\eta(t_i)$ which, by construction, have the proposed time correlation (4). However, due to the symmetries of the Fourier transform only $N/2$ of these values are actually independent and the remaining numbers are periodically correlated to them. Thus we have constructed a true random process from $t = 0$ to a maximum time $T_{cutoff} = \Delta t N/2$.

This algorithm is sufficiently general to allow generation of noise of any given correlation function. For instance, in [17] we considered Gaussian noise with a Gaussian correlation function,

$$\gamma(t) = \frac{2D}{\tau\sqrt{2\pi}} e^{-t^2/2\tau^2}$$

(10)

whose Fourier transform can be obtained analytically,

$$\widetilde{\gamma}(\omega) = 2D e^{-\tau^2\omega^2/4}.$$

(11)

According to our prescription, if we generate a discrete field of random numbers according to

$$\widetilde{\eta}(\omega_\mu) = \left[2DN\Delta t \exp\left(\frac{\tau^2}{(\Delta t)^2}(\cos(2\pi\mu/N) - 1) \right) \right]^{1/2} \alpha_\mu$$

(12)

for sufficiently large N the resulting correlation function upon Fourier inversion should match Eq. (10) (it does). Similarly, for exponentially correlated Gaussian noise, cf. Eq.(3), whose Fourier transform is

$$\widetilde{\gamma}(\omega) = \frac{2D}{1 + \tau^2\omega^2},$$

(13)

we generate the discrete random numbers according to

$$\widetilde{\eta}(\omega_\mu) = \left(\frac{2DN\Delta t}{1 + \left(\frac{2\tau}{\Delta t}\sin(\pi\mu/N) \right)^2} \right)^{1/2} \alpha_\mu$$

(14)

and again reproduce the correlation function (3) upon Fourier inversion. In both cases $2D$ is the intensity of the noise and τ its correlation time. We find that it does not matter whether we discretize the ω using the function $\cos(2\pi\mu/N)$ as in (12) or $\sin(\pi\mu/N)$ as in (14).

A more difficult noise to generate numerically is one with a memory of inverse power law form,

$$\gamma(t) = \frac{\varepsilon}{(1 + |t|/t_0)^\beta}.$$

(15)

Here t_0 is an adjustable (small) parameter. For reasons described below and related to our particular algorithm, the value of t_0 turns out to depend on β. When the power law decay exponent $\beta > 2$ then not only is the intensity of the fluctuations finite (and given by $2\varepsilon t_0/(\beta - 1)$, which increases with decreasing β), but they also have a finite correlation time (which also grows as β decreases. The effects of this sort of noise are essentially the same as those of any Gaussian noise with a finite correlation time, although direct comparison with most of the literature would have

to be done carefully [11] because correlation time effects have usually been studied in the context of noise of a fixed intensity. When $1 < \beta < 2$ then the fluctuations have a finite intensity but an infinite correlation time. We have not analyzed this case. Even more persistent correlations, and the ones of interest to us here, occur when $0 < \beta < 1$.

In order to implement the spectral method, we would first have to know the Fourier transform of the correlation function. The form (15) does not have an closed-form Fourier transform [18], and so instead we postulate or guess the form

$$\widetilde{\gamma}(\omega_\mu) = \frac{\varepsilon\beta\pi\omega_{max}^{-\beta}}{\left[\frac{2}{\Delta t}\sin(\pi\mu/N) + \omega_0\right]^{(1-\beta)}} \tag{16}$$

where ω_{max} was defined earlier as $\pi/\Delta t$ and where ω_0 is a low frequency cutoff that is chosen to control the low-frequency behavior and avoids a zero-frequency divergence. To check whether Eq. (16) is indeed an appropriate choice one has to perform the numerical inverse transform and compare with (15). For a given exponent β this comparison involves the three parameters Δt (the discretization time step), ω_0, and t_0. The value of ω_0 that leads to the best agreement turns out to depend on the time step. In our calculations we have mostly used $\Delta t = 0.01$ but in our barrier-crossing calculations in Sec. V we take $\Delta t = 0.02$. For this range of Δt we find that the best choice (giving the best concordance between the desired correlation function and the assumed Fourier transform) is $\omega_0 = 0.0001$. This is the value used throughout this analysis.
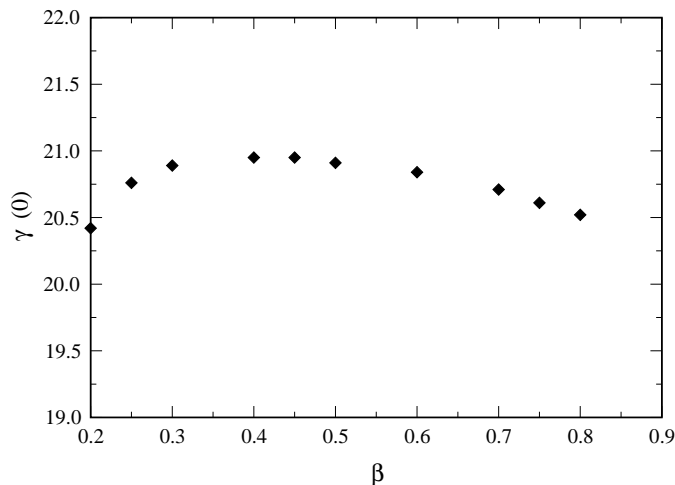

FIG. 3: $\gamma(0)$ vs β obtained from the simulations.

From Eq.(16) we obtain an important relation,

$$\gamma(0) \simeq \frac{1}{\pi}\int_0^{\omega_{max}} \widetilde{\gamma}(\omega)d\omega = \epsilon + \mathcal{O}(\omega_0/\omega_{max}), \tag{17}$$

consistent with Eq. (15). Therefore $\gamma(0)$ is independent of β and is a direct measure of the noise control parameter ε. This provides a first check for our algorithm.

A second test of our algorithm is presented in Figs. 1 and 2, where we exhibit the numerically generated correlation functions as well as the analytic counterparts with $\beta = 0.3$ and 0.6. Within the resolution of these figures, the simulated results agree well with the expected power laws given by Eq.(15) for the particular parameter choices shown in the caption. The value of ε has been assumed to be selectable independently of β and according to Eq. (17). Figure 3 shows that this is indeed the case, i.e., that $\gamma(0)$ as generated from our simulations is essentially independent of β. The small variations are due to the discreteness of the time variable and the stochasticity of the problem. More complicated is the choice of the parameter t_0: for a fixed ε, the choice of t_0 that leads to a best match between the numerically generated correlation function and the analytic form (15) depends on β, a dependence that is exhibited in Fig. 4. The parameter t_0 also varies with the time step Δt, a dependence we have not exhibited because we hold Δt fixed in our analysis. In any case, implementation of our algorithm requires attention to these dependences. The values of t_0 indicated in Figs. 1 and 1 result from this best fit.
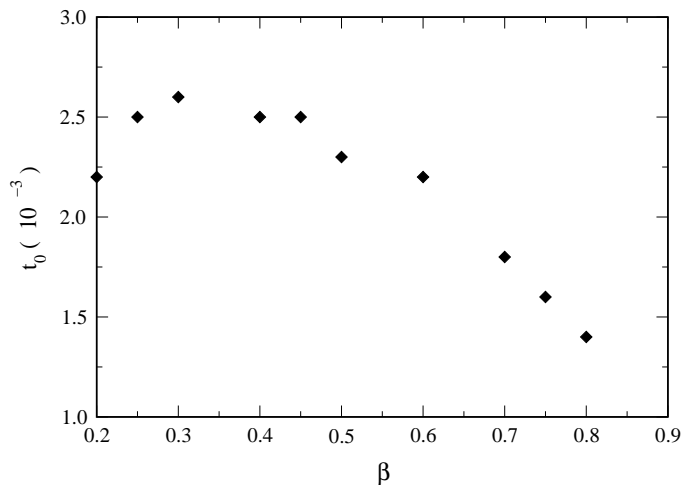
FIG. 4: Parameter t_0 found from the best fitting of the autocorrelation function Eq. (15).

β	Theory $\dfrac{2}{2-\beta}$	Simulation
0.25	1.143	1.151
0.5	1.333	1.344
0.75	1.600	1.596

TABLE I: Comparison of theoretical and simulation exponents

III. SUPERDIFFUSION OF A FREE PARTICLE

The first problem we study is of interest in the analysis of the mean exit time of a free Brownian particle from a domain bounded by absorbing walls. We consider a free particle that moves in one dimension under the influence of a long range correlated noise until it covers, on average, the distance to one of the absorbing barriers.

A dynamical equation that describes this type of dynamics is the very simple stochastic differential equation (Langevin equation)

$$\frac{dx}{dt} = \eta(t), \tag{18}$$

where $\eta(t)$ is a Gaussian power law-correlated random noise as described in section II. Note that here and in all subsequent examples we "start the clock" at $t = 0$, that is, in addition to specifying an initial value or distribution of x at $t = 0$ we also assume that the noise is "turned on" at that time. Otherwise one would need to be concerned about the role of the time $t = 0$ in the evolution of the noise, which in turn would affect the description of its correlation function.

We are particularly interested in the dependence of the mean arrival (absorption) time on the parameters β and ϵ and on the length $2L$ of the interval. The essential scaling features (exponents) of the dependences on these parameters can be obtained from a formal integration of Eq.(18), which immediately leads to the mean squared displacement relation

$$\langle x^2(t) \rangle \sim \varepsilon \, t^{2-\beta}, \tag{19}$$

characteristic of *superdiffusive* behavior [17]. Superdiffusion here arises because the arrival at the boundaries is more likely to occur via essentially ballistic motion than in the white noise case, where frequent reversals of dx/dt cause the net displacement to be slow. The time at which the mean squared displacement is proportional to L^2 can be obtained by inverting this expression. The difference between this time and the mean time $\langle T \rangle$ for *first* arrival at an absorbing boundary is due to recrossings of the boundary and only affects the prefactors, not the exponents. That is, we can use Eq. (19) to write

$$\langle T \rangle \sim \varepsilon^{-1/(2-\beta)} \, L^{2/(2-\beta)}. \tag{20}$$
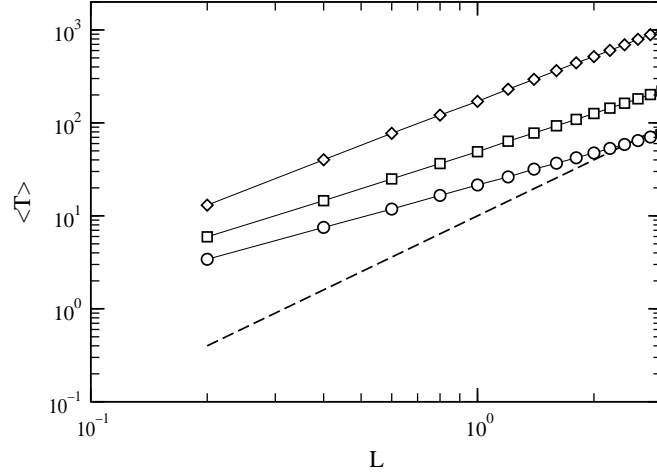
FIG. 5: Mean first passage time, $\langle T \rangle$, as function of the interval length, L, for a free particle driven by power law correlated noises with different exponents β. In all cases $\varepsilon = 0.05$. The dashed line is the theoretical prediction for white noise. The lines joining the simulation symbols are simply guides for the eye. Circles: $\beta = 0.25$; Squares: $\beta = 0.50$; Diamonds: $\beta = 0.75$. The exponents in Table I are fits to these numerical results.
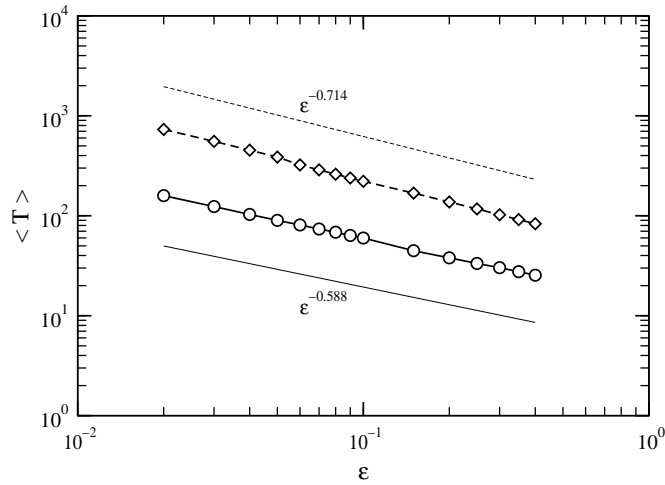

FIG. 6: Variation of the mean first passage time with ε for a free particle on an interval of length $L = 3$ and two different power laws. Circles: $\beta = 0.3$; Diamonds: $\beta = 0.6$. The exponents obtained from fitting the simulation results are 0.61 and 0.72. The auxiliary lines correspond to the theoretical exponents $(1/(2 - \beta))$, which are 0.588 and 0.714, respectively.

Note that the (Gaussian) statistics of the noise play no role in this result, which is determined entirely by the correlation function of the noise.

In order to test this theoretical prediction we have performed numerical simulations for different values of the interval length $2L$, the exponent β, and the coefficient ε. Throughout this paper all Langevin equations are numerically integrated using the Heun method, which is an extension of a second order Runge-Kutta algorithm for stochastic differential equations [19]. The results presented below are averages over 2000 realizations.

A comparison of the theoretical exponent $(2/(2-\beta))$ in Eq. (20) and the simulation results is summarized in Table I. The agreement is clearly excellent. In Fig. 5 the average exit time is presented as function of the interval length on a log-log plot. The exit time $\langle T \rangle$ follows the predicted power law behavior with the slopes of Table I. In the figure we also show the result for white noise with its characteristic exponent of 2.

Fig. 6 shows the dependence of the mean first passage time on the noise intensity parameter ε. The simulation results are in excellent agreement with the predictions of Eq. (20).
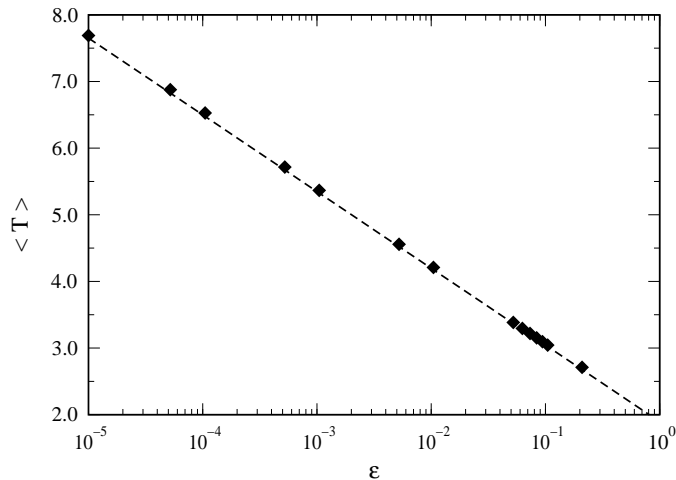
FIG. 7: Mean first passage time out of an unstable state as a function of ε for fixed $\beta = 0.5$. The dashed line is the theoretical prediction from Eq. (26) and the statistical average is over 5000 realizations.

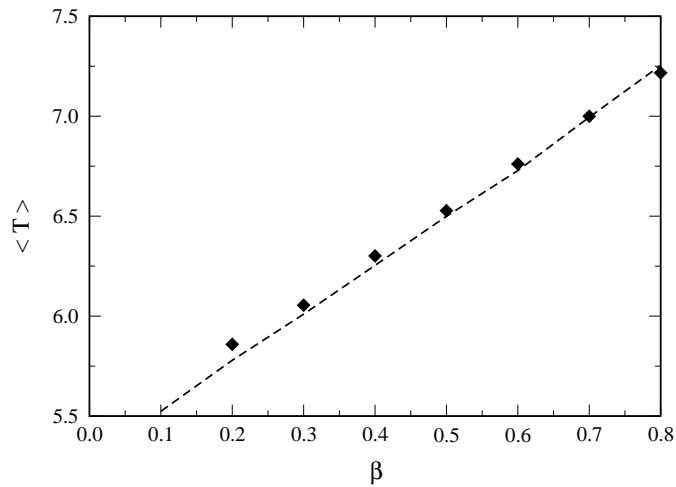FIG. 8: Mean first passage time out of an unstable state as function of the power law exponent β for fixed $\epsilon = 0.0001$. The dashed line is the theoretical prediction from Eq. (26) and the statistical average is over 5000 realizations.

IV. DECAY OF AN UNSTABLE STATE

The decay of unstable states is of course easily triggered by any disturbance, and in many physical instances the decay is caused by fluctuations. In its simplest rendition this process can be modeled by a particle initially placed at the top ($x = 0$) of an inverted parabolic potential and subject to fluctuations,

$$\frac{dx}{dt} = x - x^3 + \eta(t), \qquad x(0) = 0. \tag{21}$$

The decay at the early stages is dominated by the linear term and the fluctuations, so that in this regime the Langevin equation can be further simplified to [20]

$$\frac{dx}{dt} = x + \eta(t). \tag{22}$$

Formal integration of this linear equation immediately yields

$$x(t) = h(t)e^t, \qquad h(t) \equiv \int_0^t dt' e^{-t'} \eta(t').$$ (23)

The mean first passage time to, say, $x = \pm 1$ is identified as the time at which $\langle x^2(t) \rangle = 1$. Recrossings are even less relevant here than in the previous section; larger values of x require consideration of the nonlinear term in the evolution equation. If the time of interest is $t \gg 1$ (a condition that will be seen to be satisfied by the mean first passage time) then the upper limit in the integral in Eq. (23) can be extended to infinity, that is, we set

$$x^2(t) = h^2 e^{2t}, \qquad h = \int_0^\infty dt' e^{-t'} \eta(t').$$ (24)

Thus the fluctuations h^2 simply play the role of a random initial condition on $x^2(t)$. The random variable h has zero mean and variance σ^2 given by [21],

$$\sigma^2 = \langle h^2 \rangle = \langle \int_0^\infty dt' e^{-t'} \eta(t') \int_0^\infty dt'' e^{-t''} \eta(t'') \rangle =$$
$$\int_0^\infty e^{-2t'} dt' \int_0^\infty dt'' e^{-t''} \gamma(s) = \frac{\epsilon}{2} t_0^\beta e^{t_0} \Gamma(1-\beta, t_0).$$ (25)

The stationarity of the noise has been used to calculate the variance; $\Gamma(1-\beta, t_0)$ is the incomplete Gamma function.

The mean first passage time to $x^2 = 1$ for this process for a generic colored noise was calculated in Ref. [20]:

$$\langle T \rangle = -\frac{1}{2} \ln \left(\sigma^2 \right) + \frac{\gamma}{2},$$ (26)

where $\gamma = 0.57721...$ is the Euler constant. This result together with (25) gives an explicit expression for the mean first passage time. Figures 7 and 8 show excellent agreement between the theory and numerical simulations for the dependence of $\langle T \rangle$ on ε and on β.

V. THE BARRIER CROSSING PROBLEM

A problem that is more complex than the essentially linear ones posed so far is the "barrier crossing problem." Here we consider the diffusion of an overdamped particle in a double-well potential. The mean first passage time of interest is the time it takes the particle to go from one of the potential minima to the other when the transition is driven by power-law-correlated Gaussian fluctuations. The particle dynamics is modeled by the following Langevin equation:

$$\frac{dx}{dt} = -\frac{dV(x)}{dt} + \eta(t),$$ (27)

where the double-well potential is,

$$V(x) = -\frac{1}{2}x^2 + \frac{1}{4}x^4.$$ (28)

Our simulations follow the dynamics of each particle starting in the left well at $x(t=0) = -1.0$ until it arrives at the right well at $x(t=T) = 1.0$ for the first time. We then calculate the mean first passage time $\langle T \rangle$, that is, the average of T over many $(10,000)$ realizations.

Two questions are of interest: (1) If two noises $\eta(t)$, one δ-correlated and the other power-law correlated, lead to the same average transition time from one well to the another, are there other properties that allow a clear distinction between them? (2) For a power-law correlated noise $\eta(t)$, how does the transition time depend on the correlation function parameters? We address both of these questions below.

The numerical barrier crossing problem is fundamentally different from the problems considered in the previous section. In those, no matter how small or persistent a realization of the noise $\eta(t)$, the process $x(t)$ will eventually reach one of the boundaries of interest. How long a simulation must run in order to make sure that all processes have reached the boundaries is essentially a matter of insuring that those with the lowest value of η as given in the discretization scheme arrive there. In the barrier crossing problem, on the other hand, small-η realizations will remain
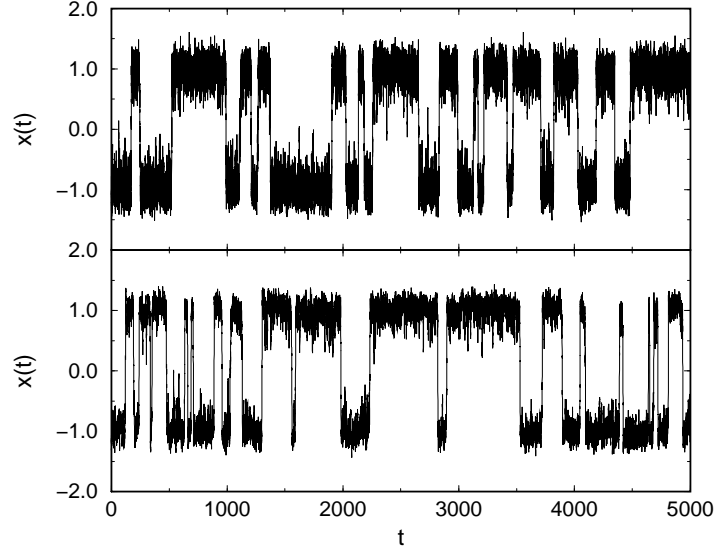
10

FIG. 9: Typical trajectories of a particle in the double well potential (27). Top panel: Gaussian white noise with $D = 0.0725$, $\langle T \rangle = 162.38$. Bottom: Gaussian power-law noise with $\beta = 0.5$, $\epsilon = 1.15$, $\langle T \rangle = 162.87$.
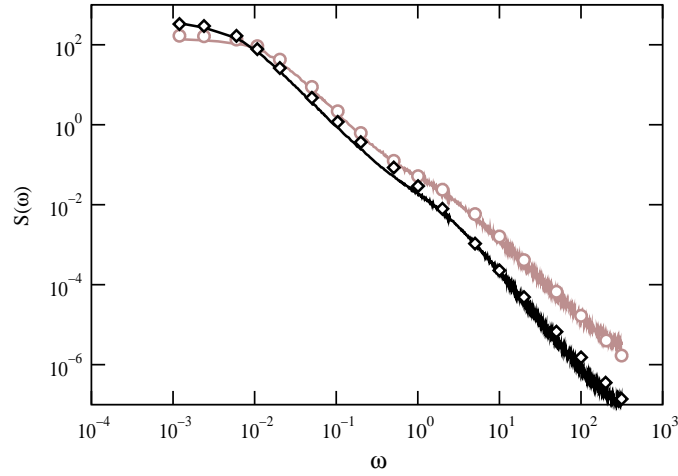

FIG. 10: Power spectra of the trajectories shown in Fig. 9 . Circles: white noise with $D = 0.0725$ and $\langle T \rangle = 162.38$. Diamonds: power-law noise with $\beta = 0.5$, $\epsilon = 1.15$ and $\langle T \rangle = 162.87$. The theoretical predictions from Eq. (31)are also included.

in one well until the value of η changes to a sufficiently high value (easy to estimate [11]) so as to effectively eliminate the barrier. The time it takes to effect this change is of course large (infinite on average) for the fluctuations considered herein. In our simulations we have carefully chosen run times that insure that all $10,000$ particles in our ensemble have made the passage from one well to the other. As we decrease ε (thus weakening the noise) and/or increase β (thus in effect also weakening the noise), the simulation time has to be increased accordingly. Note that these remarks address the *simulation* problem. A complete theory of this process would have to deal with the relative magnitudes of a number of infinities (noise intensity, noise correlation, and passage over the barrier of the slowest processes).

Fig. 9 shows two typical trajectories of the barrier crossing process for two different Gaussian noises. One is white noise, the other is power-law correlated, and the parameters have been chosen so that the mean first passage times for both are essentially the same. The effect of the long range correlations is certainly not evident from these trajectories. This observation suggests a more detailed study of the dynamical properties. The first passage time distribution and, in particular, the mean first passage time for the Gaussian white noise case, are well known analytically (see [11] and
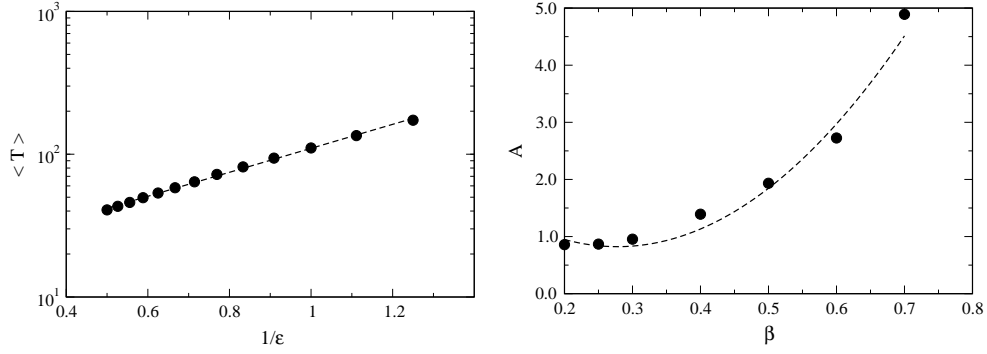
FIG. 11: First panel:Typical dependence on ε of the mean first passage time from one well to the other. The other parameters are $\beta = 0.5$, $\omega_0 = 0.0001$, and $\Delta t = 0.02$. The dashed line corresponds to $A = 1.933$. Second panel: Activation parameter A as a function of β (the value $A = 1.933$ at $\beta = 0.5$ is the result of the slope in the first panel. The dashed curve is the best numerical fit with a quadratic form, $A(\beta) = 2.42 + 11.5(1.8\beta^2 - \beta)$.
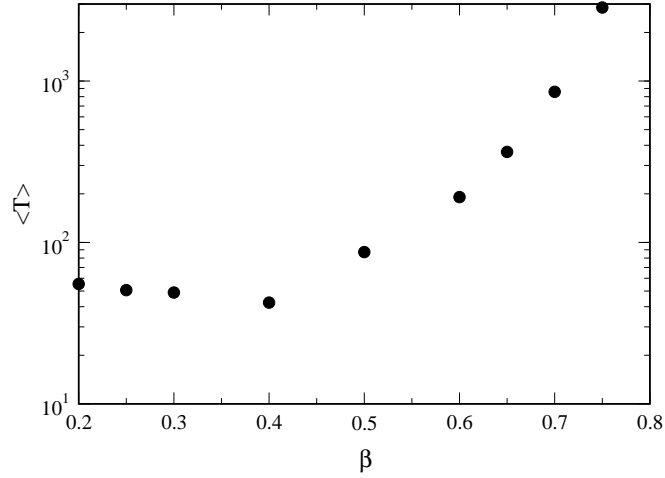

FIG. 12: Mean transition time from one well to the other as a function of β. The parameters used here are $\varepsilon = 1.15$, $\omega_0 = 0.0001$, $\Delta t = 0.02$.

the many original references therein). Approximate theories for exponentially correlated noise also abound [11], but to our knowledge there are no results for the infinite correlation time case. To deal with this problem we note that the trajectories (in either the white or the correlated noise cases) consist of two distinct components characterized by two different time scales. One component describes the rapid fluctuations in each well, and the other describes the much slower switching events between the two wells. We implement this observation by writing the trajectory $x(t)$ as a sum of these two contributions:

$$x(t) = x_D(t) + x_B(t), \tag{29}$$

where $x_B(t)$ represents the rapid random motion inside each well, and $X_D(t)$ is a dichotomous random process between the values $x = 1$ and $x = -1$, with a characteristic time controlled by the mean transition time $\langle T \rangle$. The dynamics of $x_B(t)$ can be approximated by expanding Eq. (27) around the minimum of one of the wells, e.g. as $x(t) = 1 + x_B(t)$ in the well. Then $x_B(t)$ evolves according to the Langevin equation

$$\frac{dx_B}{dt} = -2x_B + \eta(t), \tag{30}$$

which evolves on a characteristic time scale $\tau = 0.5$ that is much smaller than $\langle T \rangle$.

With this decomposition, the power spectrum of $x(t)$, denoted by $S(\omega)$, is just the sum of the spectra associated
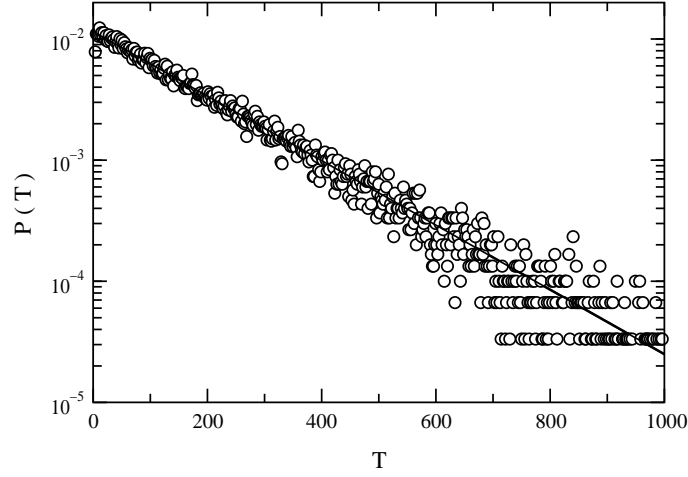
FIG. 13: Transition time probability distributions for white noise with $D = 0.0725$. The circles are the results of the simulation and the continuous line is the functions Eq. (35) with $\langle T \rangle$ obtained from the simulation data.
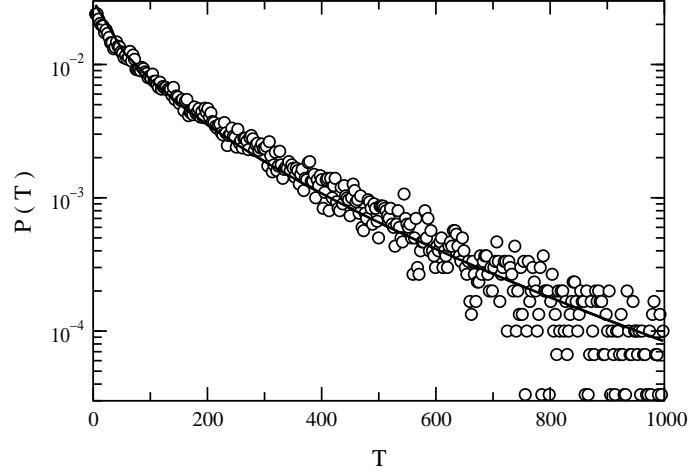

FIG. 14: Transition time probability distribution for the power law case with $\beta = 0.5, \epsilon = 1.15$. The circles are the results of the simulation and the continuous line is the function Eq. (36) with T_s, and θ obtained from the simulation data.

with $x_D(t)$ and $x_B(t)$. These can be calculated explicitly:

$$S(\omega) = \frac{4\langle T \rangle}{4 + \omega^2 \langle T \rangle^2} + \frac{\tau^2 \gamma(\omega)}{1 + \omega^2 \tau^2}. \tag{31}$$

The first contribution is the spectrum of a dichotomous process governed by the time scale $\langle T \rangle$, and the second contribution comes from the exact solution of Eq. (30) with the noise spectrum $\gamma(\omega)$. In the white noise case $\gamma(\omega) = 2D$, and for the long ranged noise the spectrum is obtained from Eq. (16) in the continuum limit,

$$\gamma(\omega) = \frac{\epsilon \beta \pi \omega_{max}^{-\beta}}{(\omega + \omega_0)^{1-\beta}} \tag{32}$$

It is interesting to note that the main difference between the white and power law spectra appear in the high-frequency (short-time) regime. In the white noise case, $S(\omega) \sim \omega^{-2}$, whereas in the correlated case we observe the more rapid decay $S(\omega) \sim \omega^{-(3-\beta)}$.

Figure 10 shows the spectra for the two trajectories shown in Fig. 9 as well as the prediction (31) for each. As noted earlier, the parameters have been chosen so as to lead to the same mean first passage time $\langle T \rangle$, but other than
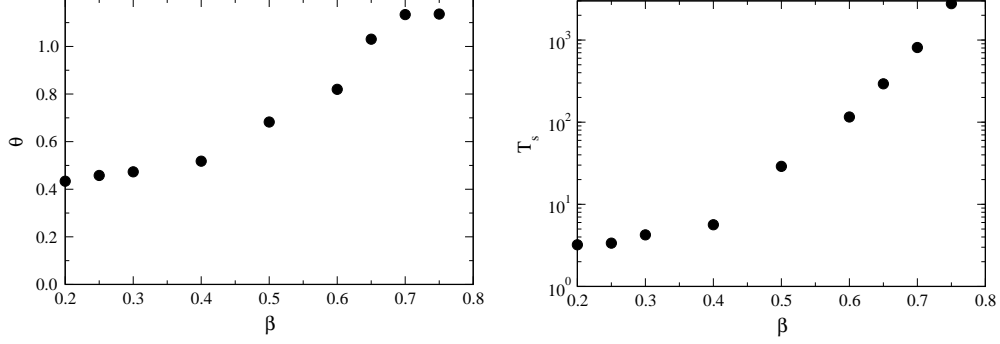
FIG. 15: First panel: Characteristic parameter θ of the stretched exponential distribution as a function of β. Secon panel: characteristic parameter T_s. The values of the other parameters are $\varepsilon = 1.15$ and $\Delta t = 0.02$.
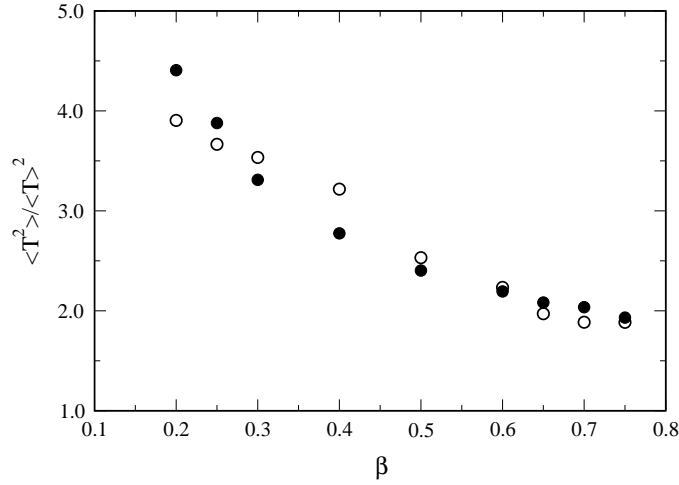

FIG. 16: Dispersion of the first passage time distribution as a function of β (full circles) compared with the proposed analytic form Eq. (38) (empty circles).

that there are no adjustable parameters. The agreement between our predictions and the numerical results is quite good in both cases. The exponent obtained from the numerical data in the high frequency regime for the correlated noise case is 2.49, which agrees with the theoretical prediction of 2.5. It is also clear that a distinction between the two types of fluctuations is difficult even at this level of detail for a given mean transition time.

In the above analysis $\langle T \rangle$ is the adjustable parameter, that is, we have fixed β and ε so as to yield a particular value of $\langle T \rangle$. The dependence of this quantity on the model parameters ε and β is yet to be explored.

The first panel in Fig. 11 is a plot of $\log\langle T \rangle$ as a function of $1/\varepsilon$. The straight line behavior shows that the transition time is described by a law of the Kramers form,

$$\langle T \rangle \sim \exp\left(\frac{A}{\varepsilon}\right). \tag{33}$$

Fitting the simulation data in the figure with a straight line we obtain $A = 1.933$, very far from the value $A = 2/27$ obtained for exponentially correlated noise [11]. We stress that the "activation parameter" A here depends on β, that is, a plot exactly like that of the first panel Fig. 11 but for a different value of β leads to a different value of A. The values of A vs β collected in this way are shown in the second panel in Fig. 11. In contrast, for noises with a finite (albeit large) correlation time A is essentially a constant independent of the noise intensity and of the correlation time. Comparison with those results is therefore not appropriate.

The dependence of the mean transition time on β qualitatively parallels that of the activation parameter but is even more complex because it is non-monotonic. The typical behavior is shown in Fig. 12. Although we have no detailed theory to account for this non-monotonicity, a qualitative explanation is possible in terms of two competing

effects, one that causes a decrease in $\langle T \rangle$ with increasing β and the other that causes $\langle T \rangle$ to increase with increasing β. At very small β the mean first passage time is dominated by those realizations of very slow passage for which $\eta(0)$ is not large enough to cause a transition and a very long wait is involved before $\eta(t)$ changes to a value that is sufficiently large. With increasing β the wait for change decreases, thus leading to faster passage. On the other hand, increasing β in effect *decreases* the intensity of the noise. To see this suppose that we calculate an effective intensity by integrating the correlation function only up to a maximum time t_{max} ($\gg t_0$), the running time of our simulations:

$$
\begin{aligned}
\int_0^{t_{max}} dt\gamma(t) &= \frac{\varepsilon t_0}{1-\beta}\left[\left(1+\frac{t_{max}}{t_0}\right)^{1-\beta}-1\right] \\
&= \frac{\varepsilon t_0}{1-\beta}\left(\frac{t_{max}}{t_0}\right)^{1-\beta}\left[1+\mathcal{O}\left(\frac{(1-\beta)t_0}{t_{max}}\right)\right].
\end{aligned}
\tag{34}
$$

The $1-\beta$ in the exponent of the large ratio t_{max}/t_0 dominates the $1-\beta$-dependence in the denominator, so that for a fixed t_{max} this decreases rapidly with increasing β. This lower effective intensity of the noise leads to slower passage. We conjecture that the interplay of the two effects leads to the non-monotonic behavior observed in Fig. 12, although the specific value and specific location of the minimum depend on ε.

In order to verify this minimum and to exhibit more information on the statistics of $\langle T \rangle$, we have also obtained numerical results for the probability distribution $P(T)$ of the exit times (of which $\langle T \rangle$ is the average). In Figs. 13 and 14 we have plotted the numerical histogram of $P(T)$ for white noise and for a power-law correlated noise, again chosen so as to correspond to the same means. The scatter of numerical points around the analytic forms discussed below (solid lines) is quite large and could be decreased by doing many more realizations for much longer times.

In the case of white noise the first passage time distribution is known to be exponential [4, 10],

$$
P(T) = \frac{1}{\langle T \rangle}\exp\left(-\frac{T}{<T>}\right).
\tag{35}
$$

Our numerical results agree with this result. For the power law case we conjecture a stretched exponential distribution for the transition time,

$$
P(T) = \frac{\theta}{T_s\Gamma(1/\theta)}\exp\left(-\left[\frac{T}{T_s}\right]^{\theta}\right),
\tag{36}
$$

where the prefactor has been chosen to ensure normalization ($\Gamma(z)$ is the Gamma function) and where the parameters θ and T_s are obtained from the simulation data. The mean first passage time in terms of these parameters is

$$
\langle T \rangle = T_s\frac{\Gamma(2/\theta)}{\Gamma(1/\theta)} = \frac{T_s}{\sqrt{2\pi}}2^{\frac{2}{\theta}-\frac{1}{2}}\Gamma(\frac{1}{\theta}+\frac{1}{2}).
\tag{37}
$$

We do not display the ε-dependence of the parameters because it is the β dependence of the first passage time that requires further understanding. Our fitting procedure for the case of $\epsilon = 1.15$ and $\Delta t = 0.02$ gives the β-dependences observed in Fig. 15. Although the dependences of the parameters on β are monotonic, the dependence of $\langle T \rangle$ on θ is not monotonic (note that T_s also varies with θ) and gives rise to the observed minimum. Using the data shown in Fig. 15 to construct $\langle T \rangle$ according to Eq. (37) one again obtains the minimum as a function of β observed in Fig. 12. Another point worth noting is the approach of the exponent θ to unity with increasing β that is seen in Fig. 15. The exponent is exactly unity for Gaussian white noise and would also be unity for $\beta > 2$.

From the proposed distribution (36) one can evaluate the second moment of the first passage time distribution. We obtain

$$
\frac{\langle T^2 \rangle}{\langle T \rangle^2} = \frac{\Gamma(1/\theta)\,\Gamma(3/\theta)}{\Gamma(2/\theta)^2},
\tag{38}
$$

For white Gaussian noise this ratio is equal to 2. We see in Fig. 16 that for correlated noise the ratio is greater than 2 reflecting the greater width of the stretched exponential distribution, but with increasing β the approach toward 2 is evident. The figure shows the moment ratio $\langle T^2 \rangle/\langle T \rangle^2$ obtained from numerical simulations (full circles) and from the analytic expression Eq. (38).

VI.   SUMMARY AND CONCLUSIONS

We have presented a numerical study and derived (in some cases) or conjectured (in others) analytic results for the first passage time problem in systems driven by long-range correlated noises. We specifically considered *Gaussian* noise, as opposed to noises with Lévy or other long-tailed distributions, or noises defined in terms of long waiting times between events, that may also lead to long-range correlations. There is an extensive literature on these non-Gaussian problems [22], but very little on the Gaussian counterpart [12, 14, 17]. We have considered highly correlated noise with an inverse power law form for the correlation function, Eq. (15), with $0 < \beta < 1$. Not only does this noise have no finite correlation time, but the correlation function is not integrable. The parameters of the problem are the exponent β and the noise control parameter ε.

First we discussed a numerical algorithm to generate this type of noise. This is in itself not a trivial problem. Then we considered several systems driven by Gaussian power-law correlated noises with a special focus on the problem of first passage to a prescribed boundary or set of boundaries. Two of these problems, the arrival of a free particle in one dimension at either end of a finite interval, and the decay of an unstable state, admit straightforward analytic solution. The dependence of the respective mean first passage times on the noise parameters were calculated explicitly and compared favorably with numerical simulations.

Our final application is more complex: Here we considered the first passage of a particle that evolves in a double well potential from one well, over the barrier, to the other well. We specifically considered two issues. One is a comparison of the trajectories of such a particle subject to Gaussian white noise and to Gaussian power-law correlated noise, with parameters chosen in such a way that the mean first passage times for crossing from one well to the other in both cases is the same. It is difficult to find a clear difference that would reveal in an experiment which type of noise the particle was subjected to. Only the high frequency decay of the respective power spectra shows some differences. The other issue we explored is the dependence of the first passage time distribution on the parameters β and ε. We found that the dependence of the mean first passage time on the noise control parameter is of the usual "activated" form, but with an effective activation parameter that depends on β. We also found that the mean first passage time exhibits a minimum as a function of β, which we explain on the basis of competing mechanisms, one of which leads to an increase of the mean first passage time with increasing β and the other to a decrease. This non-monotonicity is a signature characteristic of these fluctuations. We also found that a stretched exponential form for the first passage time distribution describes the numerical results, with a stretched exponent θ and a characteristic time T_s that both depend on β. This stretched exponential form is consistent with the non-monotonic behavior of the mean first passage time, and also gives results in agreement with the simulation outcomes for the second moment of the first passage time distribution. The stretched exponential first passage time distribution, and the dependence of the parameters of this distribution on the noise parameters ε and β, are features that have no analog in Gaussian noises with a finite correlation time.

Acknowledgements

[1] R. L. Stratonovich, *Topics in the Theory of Random Noise*, Gordon and Breach, New York (1963).
[2] N. Wax, *Selected Papers on Noise and Stochastic Processes*, Dover, New York (1954).
[3] C. W. Gardiner, *Handbook of Stochastic Methods for Physics, Chemistry, and the Natural Sciences*, Springer-Verlag, Berlin (1983).
[4] H. Risken, *The Fokker-Planck Equation: Methods of Solution and Applications*, Springer-Verlag, Berlin (1984).
[5] For a recent review see S. Redner, *A Guide to First-Passage Processes*, Cambridge University Press, Cambridge (2001).
[6] P. D. Ditlevsen, *Anomalous jumping in a double-well potential*, Phys. Rev. E **60**, 172 (1999).
[7] M Annunziato and P. Grigolini, *Stochastic versus dynamic approach to Lévy statistics in the presence of an external perturbation*, Phys. Lett. A **269**, 31 (2000).
[8] K. Lindenberg and B. J. West, *The Nonequilibrium Statistical Mechanics of Open and Closed Systems*, VCH Publishers, New York (1990).
[9] A. Montagnini, P. Allegrini, S. Chillemi, A. Di Garbo, and P. Grigolini, *Rescaling prescriptions: On the conflict between Hurst's analysis and the second moment prediction*, Phys. Lett. A **244**, 237 (1998).

[10] K. Lindenberg and V. Seshadri, *Theory of extrema. I. Asymptotic theory for Fokker-Planck processes*, J. Chem. Phys. **71**, 4075 (l979); K. Lindenberg and B. J. West, *The first, the biggest, and other such considerations*, J. Stat. Phys. **42**, 201 (1986).

[11] K. Lindenberg, B. J. West, and G. P. Tsironis, *Bistable systems driven by colored noise*, Rev. of Solid State Sci. **3**, 143 (1989) and references therein; M. Dykman and K. Lindenberg, in *Contemporary Problems in Statistical Physics*, SIAM, Ed. George H. Weiss, pp. 41-101 (1994) and references therein.

[12] H. A. Makse, S. Havlin, M. Schwartz, and H.E. Stanley, *Method for generating long-range correlations for large systems*, Phys. Rev. E **53**, 5445 (1996) and references therein.

[13] E. Koscielny-Bunde, A. Bunde, S. Havlin, E. Roman, Y. Goldreich, and H. J. Schellnhuber, *Indication of a universal persistence law governing atmospheric variability*, Phys. Rev. Lett. **81**, 729 (1998).

[14] J. García–Ojalvo and J. M. Sancho, *Noise in Spatially Extended Systems*, Springer-Verlag, New-York (1999).

[15] N-N. Pang, Y-K¿ Yu, and T. Halpin-Healy, *Interfacial kinetic roughening with correlated noise*, Phys. Rev. E **52**, 3224 (1995).

[16] A. Barabási and H. E. Stanley, *Fractal Concepts in Surface Growth*, Cambridge University Press, New York (1995).

[17] A. H. Romero and J. M. Sancho, *Generation of short and long range temporal correlated noises*, J. Comp. Phys. **156**, 1 (1999).

[18] In Ref. [12]a correlation function with the same asymptotic power law behavior but with an analytic Fourier transform is used. Since the statistical properties of interest are determined primarily by the asymptotic behavior of the correlation function, this choice would lead to similar results in our applications. However, we are interested in exploring the numerical demands of a less restricted assumption.

[19] R. Toral, in *Computational Physics, Lecture Notes in Physics* Vol.448, Springer-Verlag, Berlin, Eds. P. Garrido and J. Marro (1995).

[20] J. M. Sancho and M. San Miguel in *Noise in Nonlinear Dynamical Systems*, Cambridge University Press, Cambridge, Eds. F. Moss and P. V. E. McClintock, pp. 72-109 (1989); *ibid, Passage times for the decay of an unstable state triggered by colored noise*, Phys. Rev. A **39**, 2722 (1989).

[21] M. O. Cáceres, *Harmonic potential driven by long-range correlated noise*, Phys. Rev. E **60**, 5208 (1999).

[22] See e.g. R. Metzler and J. Klafter, *The random walk's guide to anomalous diffusion: A fractional dynamics approach*, Phys. Rep. **339**, 1 (2000) and references therein.